

## APPENDIX II.

TABLE VIII. Optical-model parameters T, from Ref. 1. All the parameters were adjusted in order to obtain the best fits to the elastic-scattering cross-section and polarization data.

Element	$V_S$ (MeV)	$r_S$ (F)	$a_S$ (F)	$W_D$ (MeV)	$r_D$ (F)	$a_D$ (F)	$V_{so}$ (MeV)	$r_{so}$ (F)	$a_{so}$ (F)	$\sigma_R$ (mb)	$\chi^2_G$	$\chi^2_P$	$N\chi^2$
<sup>48</sup> Ti	52.88	1.255	0.390	20.91	0.968	0.333	8.76	0.976	0.280	693	1.7	3.4	106
<sup>54</sup> Fe	45.61	1.306	0.701	19.37	1.370	0.293	8.68	1.284	0.359	787	0.93	1.1	48
<sup>64</sup> Ni <sup>a</sup>	50.12	1.271	0.663	12.14	1.298	0.50 <sup>b</sup>	6.31	1.285	0.50 <sup>b</sup>	966	1.4	3.3	146
<sup>68</sup> Zn	47.74	1.307	0.660	12.76	1.305	0.490	6.14	1.200	0.410	987	0.48	0.61	23

<sup>a</sup><sup>62</sup>Ni and <sup>64</sup>Zn polarization data used.<sup>b</sup>Value of parameter not adjusted by code.

\*Research sponsored by the U. S. Atomic Energy Commission under contract with Union Carbide Corporation.

<sup>1</sup>C. M. Perey, F. G. Perey, J. K. Dickens, and R. J. Silva, Phys. Rev. **175**, 1460 (1968).

<sup>2</sup>J. K. Dickens, F. G. Perey, and R. J. Silva, Oak Ridge National Laboratory Report No. ORNL-4182, 1967 (unpublished).

<sup>3</sup>F. G. Perey and G. R. Satchler, Phys. Rev. Letters **5**, 212 (1963).

<sup>4</sup>T. Tamura, Rev. Mod. Phys. **37**, 679 (1965).

<sup>5</sup>W. G. Love and G. R. Satchler, Nucl. Phys. **A101**, 424 (1967).

<sup>6</sup>J. Atkinson and V. A. Madsen, Phys. Rev. Letters **21**, 295 (1968).

<sup>7</sup>J. Delaunay, J. Passerieux, and F. G. Perey, in *Proceedings of the Second International Symposium on Polarization Phenomena of Nucleons, Karlsruhe, September 6-10 1965*, edited by P. Huber and H. Schopper (Birkhäuser Verlag, Stuttgart, Germany, 1966), p. 191, data quoted by F. G. Perey.

<sup>8</sup>W. Hauser and H. Feshbach, Phys. Rev. **87**, 366 (1952).

<sup>9</sup>R. M. Drisko (unpublished).

<sup>10</sup>P. H. Stelson and L. Grodzins, Nucl. Data **A1**, 21 (1965).

Analysis of Stripping to Quasibound Levels in <sup>41</sup>Sc<sup>†</sup>

D. H. Youngblood, R. L. Kozub, R. A. Kenefick, and J. C. Hiebert  
Cyclotron Institute, Texas A & M University, College Station, Texas 77843

(Received 2 February 1970)

Angular distributions have been measured for 15 levels observed in the <sup>40</sup>Ca(<sup>3</sup>He, d)<sup>41</sup>Sc reaction at 40-MeV bombarding energy. Distorted-wave Born-approximation calculations for the proton unstable excited states quasibound by the Coulomb and centrifugal barrier were performed using a form factor corresponding to an unbound (resonance) level in a Woods-Saxon well. The resulting spectroscopic factors are found to be insensitive to the scattering phase shifts, and in agreement with those obtained by elastic scattering. Most of the available  $1f_{7/2}$ ,  $2p_{3/2}$ , and  $2p_{1/2}$  strength and a large portion of the  $1f_{5/2}$  strength is observed below 6-MeV excitation. Little  $1g_{9/2}$  or  $2d_{5/2}$  strength is observed.

## I. INTRODUCTION

Analysis of single-nucleon transfer reactions leading to <sup>41</sup>Sc<sup>1-3</sup> has been generally limited to levels of excitation energy <2.5 MeV, because all excited states of <sup>41</sup>Sc are proton unstable, and thus distorted-wave Born approximation (DWBA) calculations may not be performed in the usual manner. We have recently studied the <sup>40</sup>Ca( $\alpha$ , t)<sup>41</sup>Sc

reaction,<sup>4</sup> but the present DWBA theory does not provide a satisfactory description of this reaction even for bound states. An analysis of the <sup>40</sup>Ca(d, n)<sup>41</sup>Sc reaction was recently reported by Gedcke *et al.*<sup>5</sup> who performed DWBA calculations for unbound levels using a modified form factor. Their technique led to spectroscopic factors which were very sensitive to the upper cutoff of the radial integrals for all but the first few levels.

The level structure of  $^{41}\text{Sc}$  has also been investigated by proton elastic scattering<sup>6,7</sup> and by proton capture<sup>8</sup> on  $^{40}\text{Ca}$ . States of low  $l$  are more easily observable in proton elastic scattering than those of high angular momentum, due to the  $l$ -dependent penetrability. For example, even if all of the  $g_{9/2}$  strength were in a single level below 3.5-MeV excitation, it would not have been observed in the elastic-scattering data of Brown.<sup>6</sup> Due to the low multipolarity of the  $\gamma$  decay to the  $\frac{7}{2}^-$   $^{41}\text{Sc}$  ground state,  $l=2, 3,$  and  $4$  capture resonances are favored in the  $^{40}\text{Ca}(p, \gamma)^{41}\text{Sc}$  reaction, and several levels are observed<sup>8</sup> at low excitation energy that are not observed in the elastic scattering.

Thus, the  $^{40}\text{Ca}(^3\text{He}, d)^{41}\text{Sc}$  reaction was investigated to obtain more information about the low-lying levels of  $^{41}\text{Sc}$ , particularly those unobserved in elastic scattering and those known to be  $l=3$  or  $4$  from proton capture. Several prescriptions for analysis of stripping to unbound levels have been presented,<sup>9,10</sup> however, these involve rather extensive computer time and programming effort, as well as an *a priori* knowledge of the phase shifts for the scattering resonance. The analysis performed here used the usual DWBA with a form factor corresponding to an unbound level obtained in a manner similar to that used for bound states. Angular momenta were known for most of the levels from previous work.<sup>3,4,6,8</sup> The spectroscopic factors are then compared with those obtained by elastic scattering.

## II. EXPERIMENTAL PROCEDURE AND RESULTS

The experimental configuration has been described earlier.<sup>4</sup> A 40-MeV  $^3\text{He}$  beam from the

Texas A & M variable-energy cyclotron, after energy analysis by a  $48^\circ$  bending magnet, bombarded a self-supporting Ca metal foil in the ORTEC 36-in. scattering chamber, and the charge was collected at a Faraday cup 1 m behind the chamber. A  $\Delta E$ - $E$  semiconductor telescope consisting of a 2-mm-thick  $\Delta E$  detector and a 3-mm-thick  $E$  detector was used to detect the deuterons with an over-all energy resolution of about 60 keV full width at half maximum. A standard particle identifier and a single-channel analyzer were used to identify and route detected deuterons into a 1024-channel segment of a multichannel analyzer. A 1200- $\mu$ -thick surface-barrier detector fixed at  $30^\circ$  served as a check on the current integrator.

Self-supporting natural calcium targets about 0.5 mg/cm<sup>2</sup> thick were prepared by vacuum evaporation. The target thickness was measured with 5.477-MeV  $\alpha$  particles and checked by comparing  $^3\text{He}$  elastic-scattering data to optical-model predictions at small angles. The over-all normalization error is estimated to be  $\pm 10\%$ . The energy scale was calculated by observing deuterons from the  $^3\text{He}$  bombardment of  $^{12}\text{C}$  and  $^{16}\text{O}$ . The beam energy and the zero angle of the chamber were determined with the cross-over technique.<sup>11</sup> Elastic scattering of 40-MeV  $^3\text{He}$  from Ca was performed to obtain optical-model parameters for the DWBA calculations.

A typical spectrum is shown in Fig. 1. The energies of 26 groups kinematically identified with the  $^{40}\text{Ca}(^3\text{He}, d)^{41}\text{Sc}$  reaction spanning the range of excitation up to 8.6 MeV were obtained with an uncertainty of  $\sim 20$  keV for most of the levels (Table I). Angular distributions were obtained for 15 of these groups for lab angles between  $10$  and  $50^\circ$  (Figs. 2 and 3). Corrections were made for con-

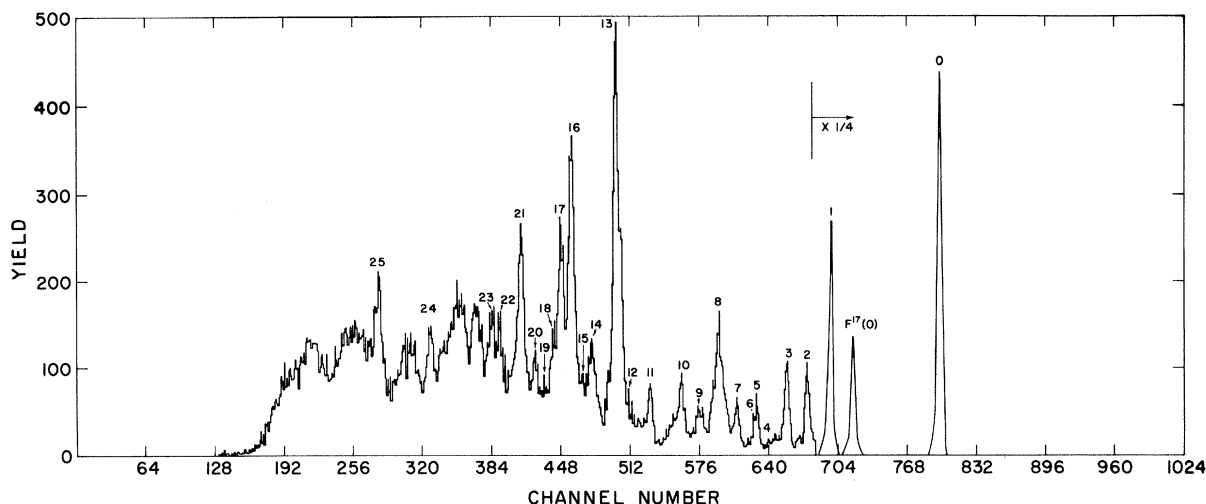


FIG. 1. Deuteron spectrum for the  $^{40}\text{Ca}(^3\text{He}, d)^{41}\text{Sc}$  reaction at a lab angle of  $25.5^\circ$ .

TABLE I. Properties of levels observed in the  $^{40}\text{Ca}(^3\text{He}, d)^{41}\text{Sc}$  reaction. The excitation energies are uncertain to  $\pm 20$  keV. The elastic-scattering spectroscopic factors were obtained from the data of Brown (Ref. 6) and Rich (Ref. 21) using the method discussed in Sec. III.B. The angular momentum and spin-parity assignments are from Refs. 1-8.

$E_x$ (MeV)	$l$	$J^\pi$	$S$	$S_{el}$	Contribution to $\sigma$ by unresolved levels
0	3	$7/2^-$	1.12		...
1.718	1	$3/2^-$	0.85	0.83	...
2.100	2	$3/2^+$	0.067		...
2.419	1	$3/2^-$	0.091	0.071	...
2.686					<20%
2.892	4	$7/2^+$	0.013		...
2.955					...
3.192	3	$5/2^-$	0.034		...
3.471	1	$1/2^-$	0.75	0.85	<1%
3.744	1	$(1/2^-)$	0.08	0.10	a
4.030	(3)	$(5/2^-)$	(0.0016-0.0070)	<0.015	b
	(4)	$(7/2^+)$	(0.0025-0.0060)	<0.29	...
4.519	4	$9/2^+$	0.015	<0.072	<25%
4.812	(3)	$(5/2^-)$	(0.0049-0.015)	<0.0033	<15%
	(4)	$(9/2^+)$	(0.00035-0.0010)	<0.036	...
5.037	4	$9/2^+$	0.18	0.17	<5%
5.413	2	$(5/2^+)$	0.031	0.072	a
5.542					b
5.709	3	$(5/2^-)$	0.15	0.11	<3%
5.862	3	$(5/2^-)$	0.060	0.07	a
5.981					a
6.157					a
6.257					a
6.470	(3)	$(5/2^-)$	(0.09)		...
6.902 <sup>c</sup>					...
7.814 <sup>c</sup>					...
8.119 <sup>c</sup>					...
8.594 <sup>c</sup>					...

<sup>a</sup>See text.

<sup>b</sup>Unresolved doublet.

<sup>c</sup>Energy uncertainty  $\pm 40$  keV.

taminant groups corresponding to levels of  $^{13}\text{N}$  and  $^{17}\text{F}$ , however, they interfered at only a few angles with a given  $^{41}\text{Sc}$  group.

### III. THEORY

#### A. DWBA Calculations

The differential cross section for a spin-zero target calculated in the DWBA is of the form<sup>12,13</sup>

$$\frac{d\sigma}{d\Omega_{ij}} = 4.42 C^2 \sigma_{ij}(\theta),$$

where  $C$  is the isotopic-spin Clebsch-Gordan coefficient [ $C=1$  for the  $(^3\text{He}, d)$  reaction on  $T=0$  targets] and  $(C^2S)$  is the usual spectroscopic factor. The reduced cross section  $\sigma_{ij}(\theta)$  is

$$\sigma_{ij}(\theta) \propto \sum_m |\beta_j^{im}|^2,$$

where

$$\beta_j^{im} \propto \iint \chi_\beta^{(-)*}(\vec{k}_\beta, \vec{r}_\beta) f_{ijm}(\vec{r}_\beta, \vec{r}_\alpha) \times \chi_\alpha^{(+)}(\vec{k}_\alpha, \vec{r}_\alpha) d\vec{r}_\alpha d\vec{r}_\beta.$$

In the zero-range approximation the form factor is given by

$$f_{ijm}(\vec{r}_\beta, \vec{r}_\alpha) \propto F_{ij}(r_\alpha) Y_l^{m*}(\theta, \phi) \delta\left(\vec{r}_\beta, \frac{M_A}{M_B} \vec{r}_\alpha\right),$$

where  $F_{ij}(r)$  is the radial wave function of the bound proton. The cross section is then obtained by representing the wave functions in the incoming and outgoing channels,  $\chi_\beta$  and  $\chi_\alpha$ , by optical-model wave functions, while  $u_{ij}(r) \equiv rF_{ij}(r)$  is calculated for a proton bound in a Woods-Saxon well. DWBA analyses of  $(^3\text{He}, d)$  and  $(d, ^3\text{He})$  reactions leading to bound final states have been re-

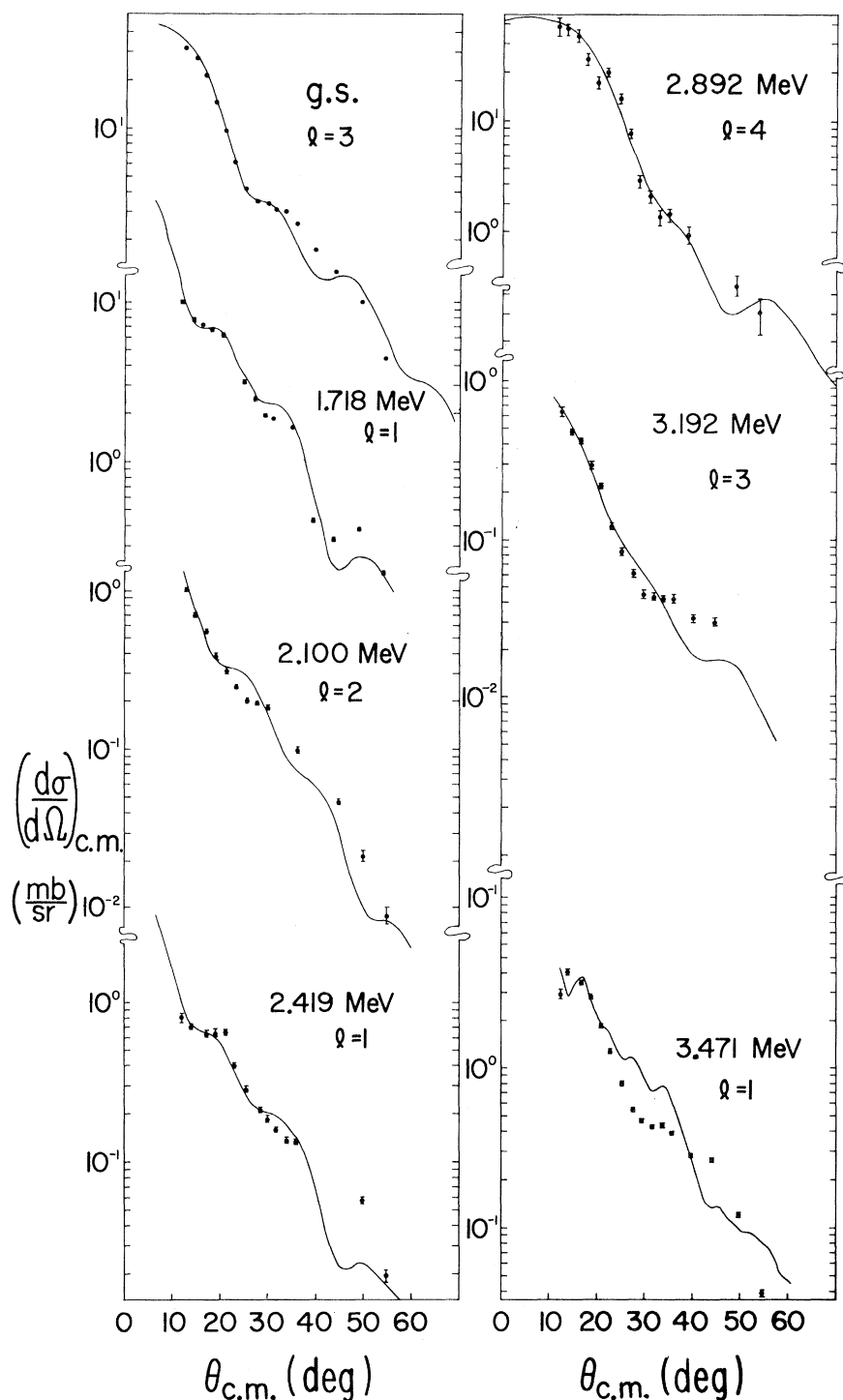


FIG. 2. Deuteron angular distributions observed in the  $^{40}\text{Ca}(^3\text{He}, d)^{41}\text{Sc}$  reaction leading to levels below 3.5-MeV excitation in  $^{41}\text{Sc}$ . The error bars refer only to statistics, and where not shown are smaller than the data points. The curves are DWBA calculations for the transitions.

ported by several authors<sup>13,14</sup> and have been reasonably successful at fitting angular distributions and obtaining consistent spectroscopic factors.

For the two-stage process,  $A + ^3\text{He} \rightarrow d + B^* \rightarrow d + p + A$ , corresponding to unbound final states;

however, the calculation is not as straightforward. Huby and Mines<sup>9</sup> have presented a technique for extending these calculations to unbound final states in the case of the  $(d, p)$  reaction. They consider reactions of the type  $C + d \rightarrow p + E^* \rightarrow p + n + C$

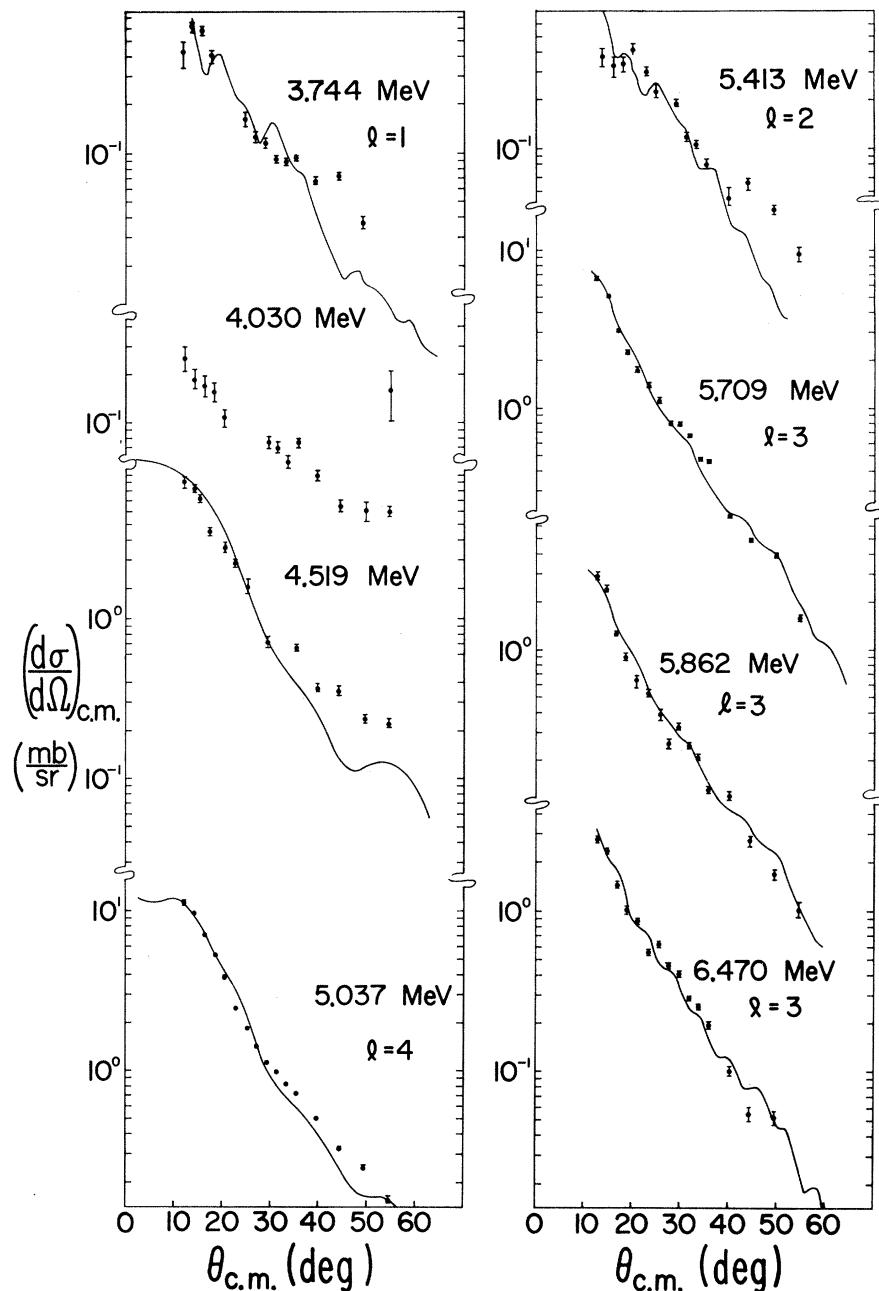


FIG. 3. Deuteron angular distributions observed in the  $^{40}\text{Ca}(^3\text{He}, d)^{41}\text{Sc}$  reaction leading to levels above 3.5-MeV excitation in  $^{41}\text{Sc}$ . The error bars refer only to statistics, and where not shown are smaller than the data points. The curves are DWBA calculations for the transitions.

and show that the matrix elements may be written in the same form as for bound states, except that the bound-state wave function for the neutron [for the  $(d, p)$  reaction] is replaced by the wave function of the  $(n + C)$  system in a scattering state. An additional integration must then be carried out over the resonance. They mention that this results in a convergent (albeit slowly) integral if the optical wave functions for the entrance and exit channels are expanded in partial

waves, as is the practice in most DWBA codes. Fortune *et al.*<sup>14</sup> have discussed the application of this technique to the  $^{12}\text{C}(^3\text{He}, d)^{13}\text{N}$  reaction, pointing out that the convergence may be slow (integration is sometimes required out to several hundred F) and that the results may be very sensitive to the exact parameters of the scattering wave function.

For the  $^{40}\text{Ca}(^3\text{He}, d)^{41}\text{Sc}$  data, however, most of the levels observed are well below the combined

Coulomb and centrifugal barrier, and might be considered quasibound (Fig. 4). Also the particle lifetimes of many of the levels observed are known from elastic scattering, and are at least 100 times longer than the orbital period of a nucleon. For bound states, the form factor may be calculated in the usual manner, while for completely unbound states, i.e., those with no significant barrier to penetrate, the scattering state wave functions may be used in the prescription of Huby and Mines, where sufficient information is available to obtain them. For states between these two extremes, technically unbound but having a high penetrability (a large barrier to penetrate), the DWBA results should be rather insensitive to the scattering phase shifts, since the shape of the wave function in the interior and surface region where the chief DWBA contribution arises is relatively insensitive to them.

A computer program was written to generate wave functions for unbound particles in a Woods-Saxon well. The depth of the well was varied to minimize the ratio of the exterior to interior amplitude of the wave function for a particle of correct  $J^\pi$  at the appropriate binding energy (negative for the unbound levels). Slight variations in this depth produce different positions for the external zero's of the wave function (different phase shifts). This form factor was read into the DWBA code DWUCK,<sup>15</sup> and calculations were then performed in the usual manner.

In the usual bound-state calculation the normalization of the bound-state wave function is

$$\int_0^\infty F_{l,j}^2(r)r^2 dr = \int_0^\infty u^2(r) dr = 1,$$

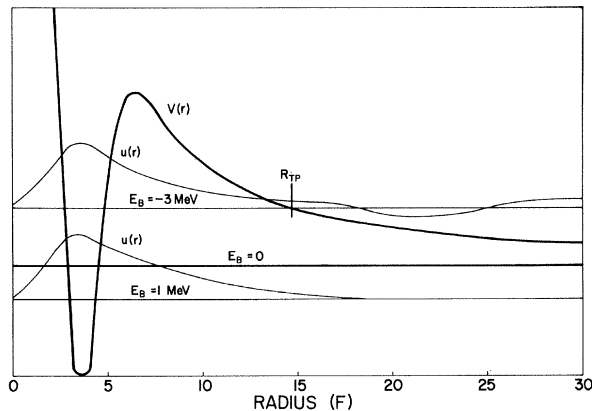


FIG. 4. The effective potential [ $V(r)$ ] for an  $l=3$  proton in a Woods-Saxon well. Also shown are qualitative sketches of the radial wave functions [ $u(r)$ ] corresponding to a bound state and a quasibound state.  $E_B$  is the proton binding energy for the level.  $R_{TP}$  is the exterior classical turning point for the unbound level shown.

where  $u(r)$  is the radial wave function for a single-particle state used to represent the bound particle in the DWBA. However, when treating an unbound wave function, the above integral is divergent. A normalization which would be finite and applicable for unbound as well as bound states is that used by Lane and Thomas<sup>16</sup> and French<sup>17</sup>

$$\int_0^a F_{l,j}^2(r)r^2 dr = \int_0^a u^2(r) dr = 1,$$

where the normalization is performed out to the channel radius  $a \equiv r_0(A_t^{1/3} + A_p^{1/3})$ , where  $A_t$  = atomic mass of the core and  $A_p$  = atomic mass of the proton. It has been shown by Lane and Thomas,<sup>16</sup> and again by Thompson, Adams, and Robson,<sup>18</sup> that taking into account the level shift  $\Delta_{\lambda\lambda}$  (in the notation of Ref. 16) in calculating reduced widths (to first order) is equivalent in the bound-state case to extending the integral to infinity (just the normalization used in the DWBA). Lane and Thomas then extend this to unbound levels where a large barrier exists by continuing the integral to the exterior classical turning point, i.e., setting

$$\int_0^{R_{TP}} u^2(r) dr = 1,$$

where  $R_{TP}$  is the classical turning point. This normalization is continuous across zero binding energy ( $R_{TP} \rightarrow \infty$  as  $E_B \rightarrow 0$ ) and results in the physically reasonable picture that the particle must be initially quasibound for the state to be formed. This normalization was adopted here for the form factor corresponding to unbound levels.

#### B. Elastic Scattering Spectroscopic Factors

The width of an isolated elastic-scattering resonance is related to the reduced width<sup>16</sup> by

$$\Gamma = 2P_l \gamma^2 / \left[ 1 - \left( \frac{\partial \Delta_{\lambda\lambda}}{\partial E} \right)_{E_r} \right], \quad (1)$$

where  $P_l$  is the Coulomb penetrability and  $\Delta_{\lambda\lambda}$  is the level shift. The reduced width,  $\gamma^2$ , is related to the radial wave function  $u(r)$  by

$$\gamma^2 = (\hbar^2/2ma)u^2(a), \quad (2)$$

where

$$a = r_0(A_t^{1/3} + A_p^{1/3}), \quad (3)$$

and  $A_t$  and  $A_p$  are the mass numbers of the target and incident particle, respectively. The radial wave function is normalized within the nuclear

interior, that is,

$$\int_0^a u^2(r) dr = 1. \quad (4)$$

If we then define

$$\gamma'^2 = \gamma^2 / \left[ 1 - \left( \frac{\partial \Delta_{\lambda\lambda}}{\partial E} \right)_{E_r} \right], \quad (5)$$

the total width may be written

$$\Gamma = 2P_1 \gamma'^2. \quad (6)$$

However Lane and Thomas<sup>16</sup> show that for bound states, the effect of the first-order energy dependence of the shift [the denominator in Eq. (1)] corresponds to setting the normalization to unity over all space, rather than to unity within the internal region. Thus

$$\left[ 1 - \left( \frac{\partial \Delta_{\lambda\lambda}}{\partial E} \right)_{E_r} \right] \approx 1 + \int_a^\infty u^2(r) dr = \int_0^\infty u^2(r) dr. \quad (7)$$

Combining (7) and (5) we have

$$\gamma'^2 = \gamma^2 / \int_0^\infty u^2(r) dr,$$

which from (2) may be written

$$\gamma'^2 = (\hbar^2/2ma)u^2(a) / \int_0^\infty u^2(r) dr,$$

or

$$\gamma'^2 = (\hbar^2/2ma)[u_z^2(a)], \quad (8)$$

where

$$\int_0^\infty u_z^2(r) dr = 1. \quad (9)$$

Lane and Thomas then argue that for unbound levels which have a large channel barrier the steps (7) and (9) above result in extension of the integral (4) to the classical turning point ( $R_{TP}$ ) rather than to infinity. Thus, for unbound levels

$$\int_0^{R_{TP}} u_z^2(r) dr = 1, \quad (10)$$

would be the appropriate normalization. The elastic-scattering spectroscopic factor is defined as<sup>18</sup>

$$S_{el} = \gamma'^2_{exp} / \gamma'^2_{s.p.} \quad (11)$$

In the work by Brown<sup>6</sup> reduced widths are given in terms of the Wigner limit

$$\gamma^2_{w.l.} = \frac{3}{2} \hbar^2 / ma^2. \quad (12)$$

Spectroscopic factors may then be determined from the results of Ref. 6 by noting that

$$\gamma'^2 / \gamma^2_{w.l.} = \frac{1}{3} a u_z^2(a). \quad (13)$$

Equation (9) also represents the normalization used for bound states in the DWBA, and (10) is the normalization adopted here for unbound levels in the DWBA. The spectroscopic factors for the elastic scattering and DWBA should then be directly comparable if the same wave function  $u(r)$  is used to represent the single-particle state for both analyses.

#### IV. DWBA ANALYSIS OF THE DATA

DWBA calculations were performed in the zero-range approximation using the computer code DWUCK by reading in an external form factor for each unbound level obtained, as discussed in Sec. III A. The optical parameters used for the entrance and exit channels are listed in Table II. The <sup>3</sup>He parameters were obtained by varying the parameters of Ridley *et al.*<sup>19</sup> to fit our 40-MeV <sup>3</sup>He elastic-scattering data with the computer code JIB.<sup>20</sup> The deuteron parameter set was obtained for 34.4-MeV deuteron scattering on calcium by Hiebert, Newman, and Bassel.<sup>13</sup> As can be seen in Figs. 2 and 3, the DWBA fits to the data are quite satisfactory for most of the <sup>41</sup>Sc levels; the poorest fits are those for the 3.471- and 3.744-MeV  $l=1$  levels and the 5.413-MeV  $l=2$  level. Due to the low angular momentum transfer, these levels are relatively weakly bound by the combined Coulomb and centrifugal barrier. The calculation reproduces the  $Q$  dependence well for the  $l=3$  levels, with good fits obtained for the ground state, as well as the known  $l=3$  levels at 5.709 and 5.862 MeV. Angular momentum assignments are difficult for the more unbound levels, due to the lack of definitive structure in the data. Spin-parity information is known for most of the levels from elastic scattering<sup>6</sup> and proton radiative capture,<sup>8</sup> as well as earlier stripping reactions.<sup>1-5</sup>

##### A. Variation of DWBA Results with Details of the Calculation

Fortune *et al.*<sup>14</sup> have indicated that the radial integrals in the DWBA calculations for unbound levels must be continued out for several hundred F to obtain convergence; otherwise the results are

TABLE II. Potential parameters used for the ( ${}^3\text{He}, d$ ) DWBA calculations.

Particle	$V$ (MeV)	$W$ (MeV)	$r$ (F)	$a$ (F)	$r_i$ (F)	$a_i$ (F)	$r_c$ (F)	$4W_s$ (MeV)
${}^3\text{He}$	177.0	14.5	1.14	0.72	1.64	0.91	1.30	
$d$	111.0		0.98	0.82	1.36	0.68	1.30	57.9
$p$			1.25	0.65			1.25	

quite sensitive to the value of the upper cutoff radius (UCO). Additionally, they found that the results were quite sensitive to the phase shifts of the wave function representing the unbound (resonance) level.

Figure 5 shows the result of varying the UCO

from 16 to 100 F for an  $l=3$  level at 5.9-MeV excitation (unbound by 4.8 MeV). Since the code DWUCK can perform a maximum of 400 integration steps, this variation was accomplished by increasing the integration step size from 0.1 F for UCO  $\leq 40$  F to 0.25 F for UCO  $> 40$  F. The principal ef-

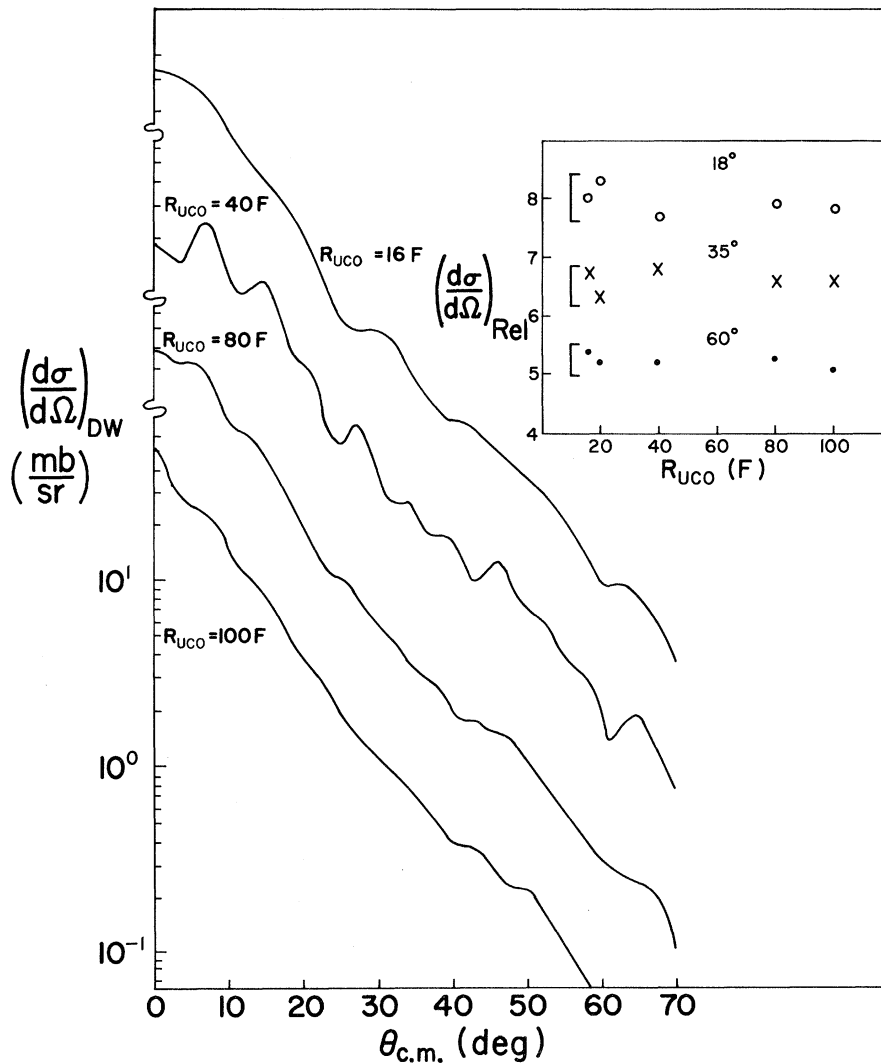


FIG. 5. Angular distributions calculated in the DWBA for an  $l=3$  transition to a level at 5-MeV excitation (unbound by 4 MeV) for several values of the upper cutoff of the radial integrals. The vertical scale has been displaced for each curve to show the shape of the curves. The inset shows the variation of the magnitude of the cross section at three angles as this upper cutoff was increased. The bars on the left are  $\pm 5\%$ . The same form factor was used for all of these calculations.



fect of increasing the UCO is to cancel out spurious high-frequency oscillations in the calculated distribution, although certain intermediate values for the UCO also result in decreasing these oscillations. However, the general slope of the distribution and the cross sections averaged over the oscillations change very little over this UCO range, so that spectroscopic factors are not affected significantly by the choice of the upper cutoff. The effect of varying the UCO is less for states more tightly bound than the  $E_x = 5.9$ -MeV level, and virtually no effect is observed on lower-energy  $l=3$  and  $l=4$  levels. For the 3.471- and 3.744-MeV  $l=1$  levels and the 5.413-MeV  $l=2$  level the effects were somewhat greater, and 100 F appeared to be insufficient as an UCO for these levels, as evidenced by the considerable spurious fine structure in the DWBA calculations shown in Figs. 2 and 3. Unfortunately a higher UCO would require increasing the integration step size beyond 0.25 F, which would be too large for an accurate calculation.

This behavior can be understood by noting that the exterior amplitude of the wave functions for these levels varies from  $\frac{1}{50}$ th of the interior amplitude for the most unbound levels to  $10^{-5}$  of the interior amplitude for those most tightly quasi-bound. For those most tightly bound, the wave function is quite similar to a bound level out to about 25–30 F, the usual UCO on radial integrals for bound states. Hence, little contribution to the reaction is expected for large  $r$ . As the level energy approaches the top of the barrier, the exterior amplitude (and hence its contribution to the

DWBA integrals) will increase. The effective barrier, which includes the centrifugal barrier [ $l(l+1)/r^2$ ], increases rapidly with increasing  $l$ . Hence, the exterior amplitudes of the wave functions for the 3.471- and 3.744-MeV  $l=1$  and 5.413-MeV  $l=2$  levels are larger than that for the 5.872-MeV  $l=3$  level, and more exterior contribution arises.

Figure 6 shows the result of varying the phase of the wave function for the 5.872-MeV  $l=3$  level by  $\frac{1}{2}\pi$  for large  $r$ . Although this produces a considerable change in the form factor for  $r > 8$  F, very little change in either the shape or magnitude of the calculated cross section results. For the 3.471- and 3.744-MeV  $l=1$  levels and the 5.413-MeV  $l=2$  level, a larger effect is evidenced, while calculations for other levels are insensitive to the phase shifts. The phase shift affects the wave function significantly only in the region within a few F of the classical turning point, which varies from 10 to 50 F for the levels observed. Since the primary DWBA contribution arises from the surface region (3–10 F) if the exterior amplitude is small, little change in the DWBA calculations results from a change in phase for all but the least-bound levels.

The cross section obtained for an  $l=3$  transfer by extrapolation from the bound region is compared with our calculation in Fig. 7. The linear extrapolation is a poor representation, and the quadratic extrapolation deviates by about 15% from the calculation at high excitation, which would result in a similar error in the spectroscopic factor. The calculation of the angular distribution for an unbound level predicts less structure and a steeper slope than for bound levels (Fig. 8), in agreement with the experimental results.

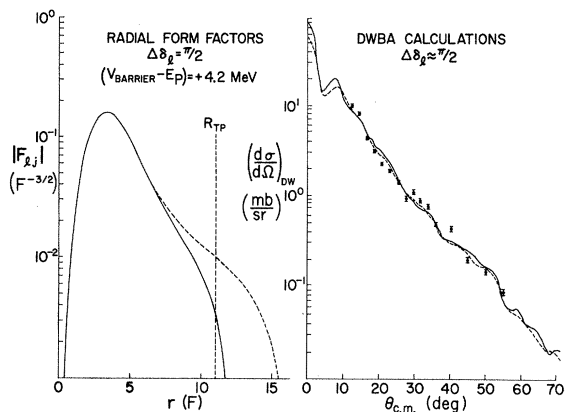


FIG. 6. (a) The radial form factor for an  $l=3$  transition for two values of the phase shift differing by  $\frac{1}{2}\pi$ .  $R_{TP}$  is the exterior classical turning point. The top of the barrier is 4.2 MeV above the position of the level ( $E_x = 5.862$  MeV). (b) The angular distributions obtained with the form factors from (a), each with the same normalization. The data for this level are normalized to the curves. An upper cutoff of 100 F on the radial integrals was used.

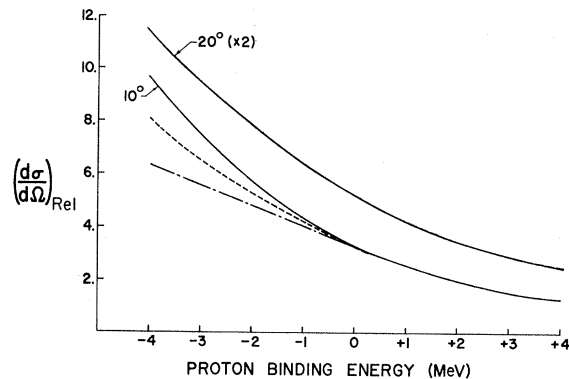


FIG. 7. The calculated DWBA differential cross section at 10 and 20° for an  $l=3$  transition as a function of the proton binding energy. The  $Q$  value was kept fixed. The dash-dot (dotted) line corresponds to a linear (quadratic) extrapolation of the calculation for bound levels at 10°. Negative binding energy corresponds to unbound (resonance) levels.

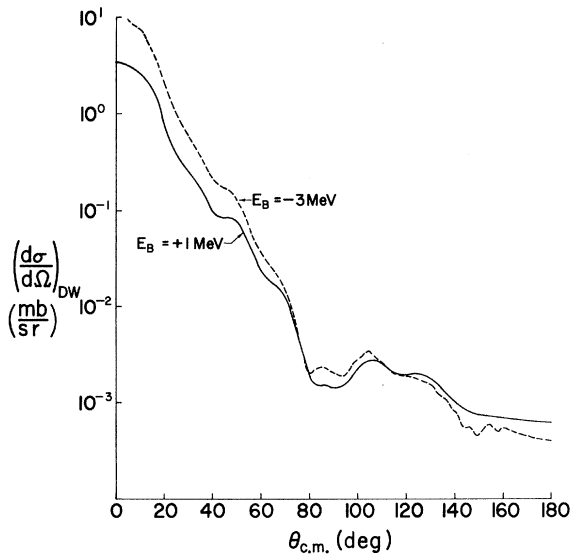


FIG. 8. Calculated angular distributions for an  $l=3$  transfer for a bound and an unbound level. The  $Q$  value is the same for both calculations.

### B. Comparison of Results with Elastic Scattering

Table III contains a list of eight  $^{41}\text{Sc}$  levels seen in the  $^{40}\text{Ca}(^3\text{He}, d)^{41}\text{Sc}$  reaction whose properties have been established by elastic-scattering experiments,<sup>6,7</sup> and which span a wide range in excitation energy and spin. As can be seen in Figs. 2 and 3, the fits to these levels of known spin and parity are satisfactory, with the exception of the least-bound levels (3.471- and 3.744-MeV  $l=1$  and 5.413-MeV  $l=2$  levels). Elastic-scattering spectroscopic factors were obtained from the data of Brown<sup>6</sup> and of Rich and Watson<sup>21</sup> using single-particle widths obtained as described in Sec. III B. Single-particle widths determined by the method

TABLE III. Comparison of spectroscopic factors obtained from the  $^{40}\text{Ca}(p, p)^{40}\text{Ca}$  (see Refs. 6 and 21) and the  $^{40}\text{Ca}(^3\text{He}, d)^{41}\text{Sc}$  reactions. The errors listed for  $S_{el}$  are due to the uncertainty in the experimental width only. The energies listed for the levels are from Ref. 6.

$E_x$ (MeV)	$l$	$J^\pi$	$\gamma'^2/\gamma_{w.l.}^2$ <sup>a</sup>	$S_{el}$	$S(^3\text{He}, d)$
1.714	1	$3/2^-$	0.45	$0.83 \pm 0.28$	0.85
2.409	1	$3/2^-$	0.028	$0.071 \pm 0.020$	0.091
3.467	1	$1/2^-$	0.32	$0.85 \pm 0.07$	0.75
3.729	1	$(1/2^-)$	0.037	$0.098 \pm 0.033$	0.08
5.036	4	$9/2^+$	0.047	$0.17 \pm 0.08$	0.18
5.416	2	$(5/2^+)$	0.022	$0.072 \pm 0.022$	0.031
5.703	3	$(5/2^-)$	0.033	$0.11 \pm 0.05$	0.15
5.872	3	$(5/2^-)$	0.020	$0.065 \pm 0.026$	0.060

<sup>a</sup>See Refs. 6 and 21.

of Schiffer<sup>22</sup> were generally in agreement with those obtained above. As can be seen from Table III, the spectroscopic factors obtained with the  $(^3\text{He}, d)$  reaction are generally in very good agreement with those obtained by elastic scattering. With the exception of the 3.467-MeV  $l=1$  and 5.416-MeV  $l=2$  levels,  $S$  values for the  $(^3\text{He}, d)$  reaction are in agreement with  $S$  values for elastic scattering to within only the elastic-scattering experimental errors, which, however, are large for some of the levels. It is generally accepted that spectroscopic factors extracted by DWBA analysis may be in error by as much as 30%,<sup>23</sup> so that the agreement between the two types of experiments is very striking.

### V. DISCUSSION

Table I lists 25 levels observed in the  $^{40}\text{Ca}(^3\text{He}, d)^{41}\text{Sc}$  reaction up to an excitation energy of 8.6 MeV, all of which may be identified with levels previously known<sup>3,8</sup> in  $^{41}\text{Sc}$ . Seven of the first ten levels observed may be identified with single  $^{41}\text{Sc}$  levels by energy alone. Most of the remaining groups may be identified with specific  $^{41}\text{Sc}$  levels by comparing their experimental  $(^3\text{He}, d)$  cross sections with those calculated using spectroscopic factors obtained by elastic scattering for each known level. The last column in Table I lists the estimated contribution to the observed cross section from weakly excited levels unresolved from the level having the major cross section in each group. Upper limits for the experimental widths of levels unobserved in the elastic scattering were taken from Fig. 16 of Ref. 6.

The primary contribution to the cross section of the 3.744-MeV group is thought to be from the known  $l=1$  level at 3.729 MeV ( $S_{el}=0.10$ ), and expected contributions from the 3.769-MeV ( $l=1, S_{el}=0.005$ ) and 3.779-MeV ( $l=2, S_{el}=0.01$ ) levels have been taken into account in determining  $S$ . The groups at 4.030 and 5.542 MeV contain contributions of unknown strengths from at least two known levels. The 4.519- and 4.812-MeV levels are each indicated to be  $(\frac{3}{2}^-, \frac{3}{2}^+)$  by the  $^{40}\text{Ca}(p, \gamma)^{41}\text{Sc}$  reaction.<sup>8</sup> An  $l=4$  calculation results in a slightly better fit to the 4.519-MeV level than does an  $l=3$ , and the spectroscopic factor obtained for  $l=3$  ( $S=0.030$ ) is a factor of 6 larger than the upper limit indicated by Brown ( $S_{el} < 0.005$ ), whereas the  $l=4$  spectroscopic factor ( $S=0.015$ ) is less than his upper limit ( $S_{el} < 0.072$ ). Therefore, the 4.519-MeV level appears to be  $l=4, \frac{3}{2}^+$ . Estimates of the  $(^3\text{He}, d)$  spectroscopic factor for the 4.812-MeV level are well below the elastic-scattering limit for  $l=4$ , and sufficiently close to the limit for  $l=3$  to prevent a reliable  $J^\pi$  assignment for this state.

The group at 5.413 MeV may contain contributions from six known levels, but the primary contributions are expected to be from the 5.416-MeV  $l=2$  level ( $S_{el}=0.072$ ) and the 5.371-MeV  $l=2$  level ( $S_{el}=0.029$ ), with smaller contributions from the  $l=1$  levels at 5.392-MeV ( $S_{el}=0.005$ ) and 5.490-MeV ( $S_{el}=0.10$ ). The spectroscopic factor obtained for the 5.416-MeV  $l=2$  level (0.031) assumes relative excitation of the above levels as indicated by their elastic-scattering spectroscopic factors. Several levels may be contributing to each of the groups observed above 5.8 MeV, however a major portion of the 5.862-MeV group appears to be due to the known<sup>6</sup>  $l=3$  level at 5.872 MeV, while a pair of known<sup>7</sup>  $l=3$  levels at 6.434 and 6.468 MeV appear to be the major components of the 6.470-MeV group.

## VI. SUMMARY AND CONCLUSIONS

The present DWBA analysis of stripping to <sup>41</sup>Sc levels quasibound by the Coulomb and centrifugal barriers has led to acceptable fits to the (<sup>3</sup>He, *d*) data, and to spectroscopic factors in agreement with those obtained from elastic scattering for angular momentum transfers from  $l=1$  to  $l=4$  over the range of excitation from 1 to 6 MeV. Angular momentum assignments would, however, not be possible except for the first few levels, because of the lack of definitive structure in the data. The form factors for the unbound levels were obtained from a Woods-Saxon well with the eigenfunction condition requiring a minimum in the ratio of exterior to interior amplitudes. This simple approximation, with the form factor normalized to unity at the exterior classical turning point, leads to DWBA results which are relatively independent of the upper cutoff on the radial integrals and the phase of the bound-state wave function when the exterior contribution is small, which occurs when the exterior amplitude ( $F_{lj}$ ) is less than about 1% of the interior amplitude.

Levels in <sup>41</sup>Sc representing components of six major single-particle shells are observed in the <sup>40</sup>Ca(<sup>3</sup>He, *d*)<sup>41</sup>Sc reaction. The ground state contains the major fraction of the  $1f_{7/2}$  strength, while the 1.718- and 2.419-MeV  $J^\pi = \frac{3}{2}^-$  levels contain most of the  $2p_{3/2}$  strength ( $S=0.94$ ). The energies

and spectroscopic factors of these two levels, as well as their decay properties, are described by both Gerace and Green<sup>24</sup> and Federman, Greek, and Osnes.<sup>25</sup> The levels at 3.471 and 3.744 MeV contain a large portion of the  $2p_{1/2}$  strength ( $S=0.83$ ).

A fraction of the  $1f_{5/2}$  strength is observed in the 3.192-, 5.709-, and 5.862-MeV levels ( $S=0.24$ ), while Brown has obtained  $S=0.035$  for an  $l=3$  level at 4.950 MeV. Marinov *et al.*<sup>7</sup> have investigated the region of excitation from 5.8 to 7.2 MeV in <sup>41</sup>Sc by <sup>40</sup>Ca(*p, p*)<sup>40</sup>Ca, and have found 11 levels having  $l=3$  which can account for additional  $1f_{5/2}$  strength ( $S=0.37$ ), while Rich<sup>26</sup> has observed 12  $l=3$  levels with a total spectroscopic strength  $S=0.16$  in the excitation region from 7.1 to 8.2 MeV, again with the <sup>40</sup>Ca(*p, p*)<sup>40</sup>Ca reaction. Thus if all of the  $l=3$  strength up to 8.2-MeV excitation (excluding the ground state) is attributed to the  $f_{5/2}$  shell, one can account for approximately 80% of the  $1f_{5/2}$  strength.

The levels at 4.519 and 5.037 MeV contain about 20% of the expected  $1g_{9/2}$  strength. Marinov *et al.*<sup>7</sup> found only four  $l=4$  levels with a total strength  $S=0.006$  from 5.8 to 7.1 MeV, while Rich<sup>26</sup> has observed one  $l=4$  level at 7.563 MeV with  $S=0.042$ . If all of these are attributed to the  $g_{9/2}$  shell, only 25% of the strength is accounted for by known levels below 8.3 MeV.

If the 5.413-MeV  $l=2$  level has spin  $\frac{5}{2}^+$ , as preferred by Brown, it represents only 3 to 7% of the  $2d_{5/2}$  single-particle strength, whereas Marinov and Rich observe  $l=2$  levels with about 15% of the  $d_{5/2}$  strength (if they are all attributed to the  $2d_{5/2}$  shell) between 5.8 and 8.3 MeV. Other known  $\frac{5}{2}^+$  levels below 5.8 MeV contain about 6% of the single-particle strength. Thus a maximum of about 30% of the  $2d_{5/2}$  strength could be accounted for below 8.3 MeV. Also, the absence of the  $E1$   $\gamma$  transition to the ground state in the (*p,  $\gamma$ )* reaction<sup>8</sup> indicates the possibility of a  $\frac{3}{2}^+$  assignment for the 5.413-MeV level, which would leave the  $\frac{5}{2}^+$  strength split among several weak levels.

## ACKNOWLEDGMENT

The authors are indebted to Dr. W. A. Pearce for many helpful discussions.

†Work supported by the U. S. Atomic Energy Commission and the Robert A. Welch Foundation.

<sup>1</sup>B. E. F. Macefield, J. H. Towle, and W. B. Gilboy, Proc. Phys. Soc. (London) **77**, 1050 (1961).

<sup>2</sup>H. E. Wegner and W. S. Hall, Phys. Rev. **119**, 1654 (1960).

<sup>3</sup>R. Bock, H. H. Duhm, and R. Stock, Phys. Letters **18**, 61 (1965).

<sup>4</sup>D. H. Youngblood, R. L. Kozub, R. A. Kenefick, and J. C. Hiebert, Nucl. Phys. **A143**, 512 (1970).

<sup>5</sup>D. A. Gedcke, S. T. Lam, S. M. Tang, G. M. Stinson, J. T. Sample, T. B. Grandy, W. J. McDonald, W. K.

- Dawson, and G. C. Neilson, Nucl. Phys. **A134**, 141 (1969).
- <sup>6</sup>N. A. Brown, Ph. D. thesis, Rice University, 1963 (unpublished); N. A. Brown and C. M. Class, Bull. Am. Phys. Soc. **8**, 127 (1963).
- <sup>7</sup>A. Marinov, C. Drory, E. Navon, J. Burde, and G. Engler, Phys. Rev. Letters **23**, 23 (1969).
- <sup>8</sup>D. H. Youngblood, B. H. Wildenthal, and C. M. Class, Phys. Rev. **169**, 859 (1968).
- <sup>9</sup>R. Huby and J. R. Mines, Rev. Mod. Phys. **37**, 406 (1965).
- <sup>10</sup>F. S. Levin, Ann. Phys. (N.Y.) **46**, 41 (1968).
- <sup>11</sup>B. M. Bardin and M. E. Rickey, Rev. Sci. Instr. **35**, 102 (1964).
- <sup>12</sup>G. R. Satchler, Nucl. Phys. **55**, 1 (1964).
- <sup>13</sup>J. C. Hiebert, E. Newman, and R. H. Bassel, Phys. Rev. **154**, 898 (1967).
- <sup>14</sup>H. T. Fortune, T. J. Gray, W. Trost, and N. R. Fletcher, Phys. Rev. **179**, 1033 (1969).
- <sup>15</sup>P. D. Kunz, private communication.
- <sup>16</sup>A. M. Lane and R. G. Thomas, Rev. Mod. Phys. **30**, 257 (1958).
- <sup>17</sup>J. B. French, in *Nuclear Spectroscopy*, edited by F. Ajzenberg-Selove (Academic Press Inc., New York, 1960), Part B, p. 890.
- <sup>18</sup>W. J. Thompson, J. L. Adams, and D. Robson, Phys. Rev. **173**, 975 (1968).
- <sup>19</sup>B. W. Ridley, E. F. Gibson, J. J. Kraushaar, M. E. Rickey, and R. H. Bassel, Bull. Am. Phys. Soc. **11**, 118 (1966).
- <sup>20</sup>Received from F. G. Perey, Oak Ridge National Laboratory.
- <sup>21</sup>W. F. Rich and C. E. Watson, to be published.
- <sup>22</sup>J. P. Schiffer, Nucl. Phys. **46**, 246 (1963).
- <sup>23</sup>L. L. Lee, Jr., in *Proceedings of the International Conference on Nuclear Physics, Gatlinburg, Tennessee, 12-17 September 1966*, edited by R. L. Becker and A. Zucker (Academic Press Inc., New York, 1967), pp. 31-46.
- <sup>24</sup>W. J. Gerace and A. M. Green, Nucl. Phys. **A93**, 110 (1967).
- <sup>25</sup>P. Federman, G. Greek, and E. Osnes, Nucl. Phys. **A135**, 545 (1969).
- <sup>26</sup>W. F. Rich, Ph. D. thesis, Rice University, 1967 (unpublished).

## Proton Total Reaction Cross Sections in the 10–20-MeV Range: Calcium-40 and Carbon-12<sup>†</sup>

J. F. Dicello\* and G. Igo‡

*University of California, Los Alamos Scientific Laboratory, Los Alamos, New Mexico 27544*  
(Received 2 February 1970)

Total reaction cross sections for protons on <sup>40</sup>Ca have been measured at 15 energies between 10.3 and 21.6 MeV by the beam-attenuation method. The total reaction cross section for <sup>40</sup>Ca rises sharply at low energies, reaches a maximum value around 13 MeV, and reaches a minimum value around 16 MeV. The rise at the lower energies is a result of the Coulomb barrier. The dip at 16 MeV is probably associated with the (*p, n*) threshold for <sup>40</sup>Ca. A comparison is made between the present experimental values and preliminary optical-model predictions based on available elastic-scattering data and polarization data. The variation in the reaction cross section is also compared with the integrated partial cross sections for elastic scattering. Total reaction cross sections for protons on carbon have been measured at ten energies between 9.88 and 19.48 MeV. Resonances in the total reaction cross section are observed in the neighborhood of 10.4 and 13.8 MeV. Variations of 200 mb are seen in the cross sections with changes in energy of the incident protons of about 200 keV. A comparison is made of the present total reaction cross sections and the integrated partial cross sections for elastic scattering and inelastic scattering to the first excited state of <sup>12</sup>C.

### I. INTRODUCTION

There exists a limited amount of data<sup>1,2</sup> regarding the variation of the total reaction cross section as a function of energy. Such data are necessary for determining optical-model parameters over a particular range of energies. Measurements for <sup>40</sup>Ca and <sup>12</sup>C of this kind are presented in this paper. The differential elastic cross sections for <sup>40</sup>Ca in the same energy region also have been

measured.<sup>3</sup> Polarization data for <sup>40</sup>Ca in the same region have been obtained by Baugh *et al.*,<sup>4</sup> Rosen *et al.*,<sup>5</sup> and Bercaw and Boschitz.<sup>6</sup>

Considerable information regarding differential cross sections for carbon is available<sup>7-15</sup> in the region from 9 to 20 MeV. However, only a limited amount of data is available for proton total reaction cross sections,  $\sigma_R$ , in the same region. Makino, Waddell, and Eisberg<sup>16</sup> have examined the total reaction cross section of <sup>12</sup>C as a function of